Invited paper presented at 195th Electrochemical Society Meeting, Seattle WA, May 1999. Proc. Symp. 30th State-of-the-Art Program on Compound Semiconductors, **99-4**, 1-12, Electrochemical Society, Pennington, NJ (1999).

INDUCTIVELY-COUPLED PLASMA DEPOSITION OF LOW TEMPERATURE SILICON DIOXIDE AND SILICON NITRIDE FILMS FOR III-V APPLICATIONS

K. D. Mackenzie, J. W. Lee, and D. Johnson
Plasma-Therm, Inc.
10050 16th Street N., St. Petersburg, FL 33716, USA

Low temperature SiO_2 and SiN_x films have been prepared in an inductively-coupled plasma (ICP) reactor. The material properties of these films have been investigated as a function of ICP source power, rf chuck power, reactor pressure, gas chemistry, and process temperature. The SiO_2 and SiN_x films were prepared from gas mixtures of (SiH_4 + O_2) and (SiH_4 + N_2 + Ar), respectively. A series of SiO_2 and SiN_x films were also prepared by plasma-enhanced chemical vapor deposition (PECVD) from gas mixtures of (SiH_4 + N_2O + N_2) and (SiH_4 + NH_3 + N_2). For process temperatures of less than 200 °C, the results indicate that films prepared in an ICP reactor are of improved quality. Selected properties from this work as a function of reactive gas ratio and rf chuck power are presented and discussed.

INTRODUCTION

Plasma-deposited SiO_2 and SiN_x films are widely used in the fabrication of III-V semiconductor devices [1,2]. Some specific applications are surface passivation, capacitor and interlevel dielectric, hard mask for pattern transfer, and cap layer for high temperature annealing. For these applications, high quality films deposited at low temperatures that are stable and of low hydrogen content are required. Hydrogen incorporation is inevitable as the films are typically prepared from hydride source gases such as SiH_4 and NH_3. Plasma damage during the deposition (or etch) process, resulting in physical and electronic degradation of the III-V device is also an important issue [3-11].

The conventional technique to grow SiO_2 and SiN_x films is by plasma-enhanced chemical vapor deposition (PECVD). Low temperature films prepared by this method can contain significant amounts of hydrogen. These films can also be of inferior structural and electronic quality. In recent years, there has been a growing interest in an alternative deposition technique, high-density plasma chemical vapor deposition (HDPCVD). Several different types of high-density plasma sources are available [12,13] such as electron-cyclotron resonance (ECR), helicon resonator, and the inductively-coupled plasma (ICP). HDPCVD offers the possibility of improved film quality at reduced process temperatures [14-19]. The focus in this paper is on a study of low temperature HDPCVD SiO_2 and SiN_x films prepared in an inductively-coupled plasma (ICP) reactor.

EXPERIMENTAL

All the SiO_2 and SiN_x films were prepared in a Plasma-Therm HDPCVD Versalock® reactor. Figure 1 details the essential features of the reactor. An inductively coupled plasma (ICP) source operating at 2 MHz generates the high-density plasma (> 10^{11} cm^{-3}). A separate rf supply operating at 13.56 MHz is applied to the wafer chuck. A ceramic clamp mechanically holds the wafer on the chuck. An oil recirculating heat exchanger connected to the chuck controls the wafer temperature. Helium backside cooling of the wafer is used for efficient heat transfer. The process temperature can be controlled between about 50 to 300 °C.

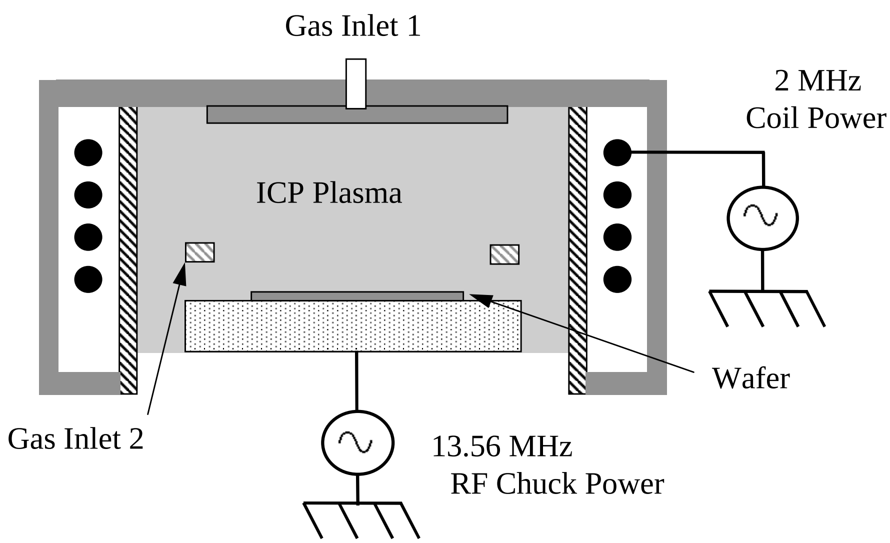

Figure 1. Schematic diagram showing the ICP source of the HDPCVD reactor.

The process gases are injected into the reactor via the ICP source (Inlet 1) and via a gas distribution ring (Inlet 2) at the wafer plane. The gas ring uniformly distributes the SiH_4 across the wafer surface. The source gases were O_2 for SiO_2, and N_2 and Ar for SiN_x. A high conductance chamber and vacuum system design enables the ability to flow these process gases at relatively high rates while maintaining the low process pressures of 2 to 10 mTorr necessary to sustain the high-density plasma.

The SiO_2 films were deposited at 100 °C. The ICP source power and process pressure were 400 W and 10 mTorr, respectively. The O_2 / SiH_4 ratio was varied from 0.75 to 2, while the SiH_4 gas flow rate and rf chuck power were held constant at 40 sccm and 50 W, respectively. At a fixed O_2 / SiH_4 ratio of 1.3, the rf chuck power was varied from 0 to 350 W. The SiH_4 gas flow rate was 50 sccm. The SiN_x films were deposited at 150 °C. The ICP source power and the process pressure were held fixed at 800 W and 10 mTorr, respectively. The total gas flow was 42 sccm and the Ar flow was 20 sccm. The N_2 / SiH_4 ratio was varied from 0.5 to 0.95, while the rf chuck power was held constant at 120 W. At a fixed N_2 / SiH_4 ratio of 0.7, the rf chuck power was varied from 25 to 150 W.

For this study, all the films were deposited on 4 inch Si wafers. The typical thickness of the films was 1000 to 5000 Å. Depositions have also been done on InP and GaAs test wafers. The deposited films were characterized by refractive index, stress, deposition rate, deposition uniformity, and wet-etch rate. A Gaertner model L116D-PC ellipsometer was used to determine the refractive index. The film thickness and thickness uniformity were measured optically with a NanoSpec model 4150 metrology system. A buffered HF (BHF) etch solution of 7:1 NH_4 : HF was used for the wet-etch rate measurements. The wafer bow technique was used to determine the intrinsic film stress of the deposited film. The measurements were made on a Tencor model P-2 long scan profiler.

RESULTS AND DISCUSSION

Silicon Dioxide

In this section, the results are presented of a study on the effects of O_2 / SiH_4 gas ratio and rf chuck power on the material properties of SiO_2. The particular properties investigated were deposition rate, stress, refractive index, and BHF etch rate. The refractive index and BHF etch rate provide important information on the stoichiometry and the homogeneity of the deposited films. Films with a refractive index of between 1.46 to 1.48, a low BHF etch rate, and a low compressive stress are desirable.

The reactions involved during any plasma deposition process are exceedingly complex; the deposition of SiO_2 from the interaction of SiH_4 and O_2 being no exception [20,21]. However, the principal reactions that promote film growth may be summarized by the following three equations [22,23]:

$$2O_2 + SiH_4 \rightarrow SiO_2{:}(OH) + nH_2O \qquad (1)$$

$$O_2 + SiH_4 \rightarrow SiO_2 + 2H_2 \qquad (2)$$

$$O_2 + 2SiH_4 \rightarrow SiO_2{:}H + nH_2 \qquad (3)$$

Examination of these equations reveals that the ratio of O_2 to SiH_4 has a significant impact on both the stoichiometry and the quality of the SiO_2 film deposited from the plasma. Figures 2, 3, and 4 summarize the dependence of the film properties on the O_2 / SiH_4 ratio. The deposition rate was about 1300 Å/min. The thickness uniformity was ±2.5 % across the wafer.

The responses shown in Figures 2 and 3 for the refractive index and the BHF etch rate are in agreement with the expectations based on the reaction equations discussed above. According to the refractive index data, for O_2 / SiH_4 ratios of lower than about 1.25, the oxide films are of high index and most likely Si rich. For ratios of 1.25 and higher, the refractive index is 1.47 and independent of the ratio. The BHF etch rate increases dramatically with increasing gas ratio. Beyond a ratio of 1.5, the BHF etch rates are over 4000 Å/min. From these results, the optimum O_2 / SiH_4 ratio is about 1.25. From Figure 4, the general trend in film stress is an increase with decreasing O_2 / SiH_4 ratio. The stress is about 300 MPa, compressive for the optimum O_2 / SiH_4 ratio of about 1.25.

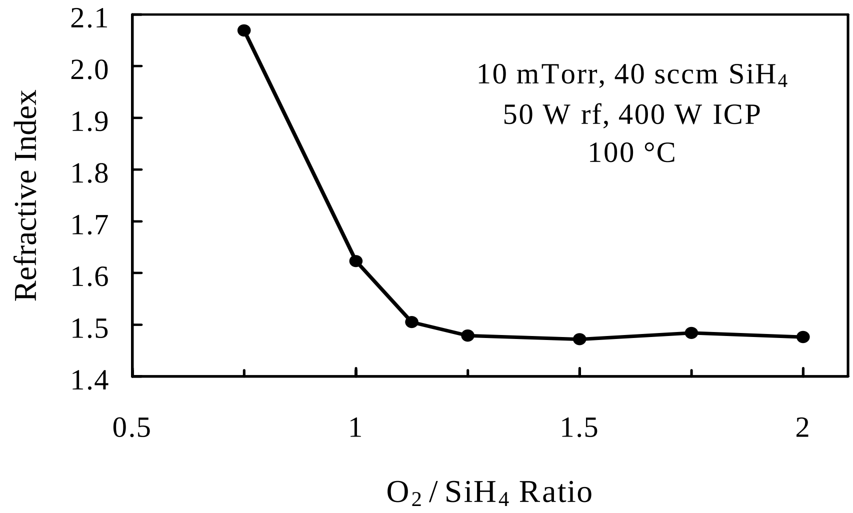

Figure 2. Refractive index of HDPCVD oxide as a function of O_2 / SiH_4 ratio.

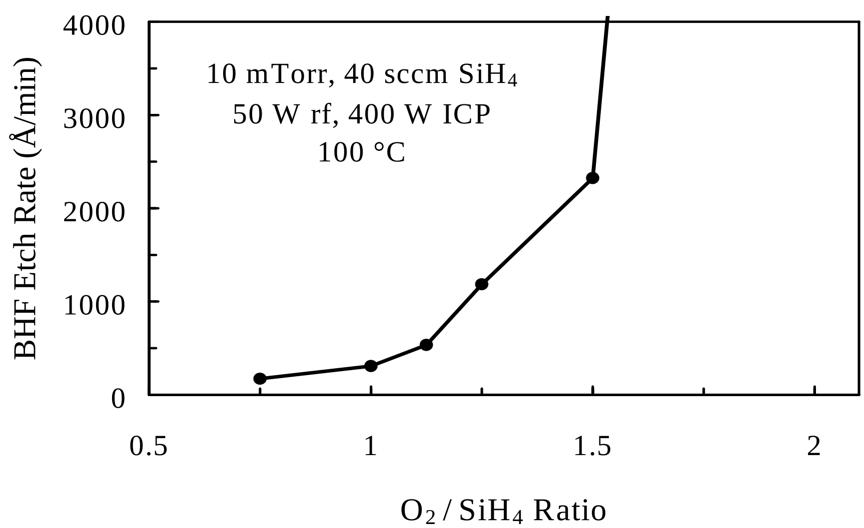

Figure 3. Variation of wet-etch rate of HDPCVD oxide with O_2 / SiH_4 ratio.

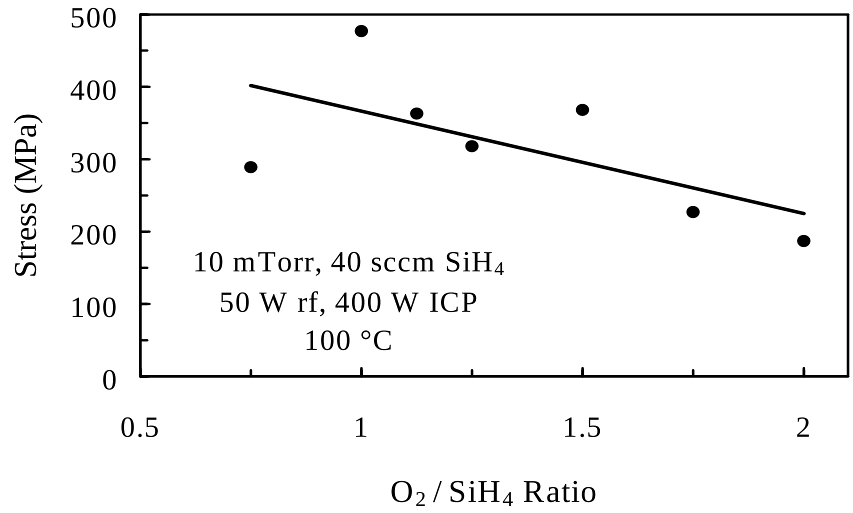

Figure 4. Film stress of HDPCVD oxide as a function of O_2 / SiH_4 ratio. The stress is compressive for all films.

Figures 5, 6, and 7 summarize the effect of rf chuck power on the measured film properties. All the films were deposited using the optimum O_2 / SiH_4 ratio of 1.3. The most significant result from these data is the important role that rf chuck power plays in achieving high quality films at such low deposition temperatures. With the addition of only 50 W rf chuck power, the BHF etch rate is reduced from about 30,000 Å/min at zero chuck power to about 1300 Å/min. The film stress also becomes more compressive. This suggests that the main effect of rf chuck power is to densify the growing film. The monotonic reduction in deposition rate with increasing rf chuck power (Figure 7) is probably a sputtering effect due to increased ion bombardment. Similar results have been reported for SiO_2 films deposited by ECR [23].

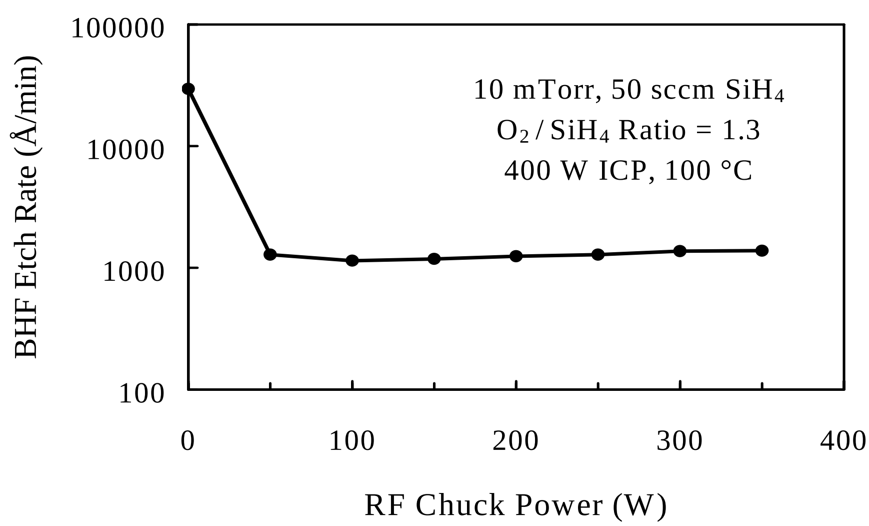

Figure 5. Variation of wet-etch rate of HDPCVD oxide with rf chuck power.

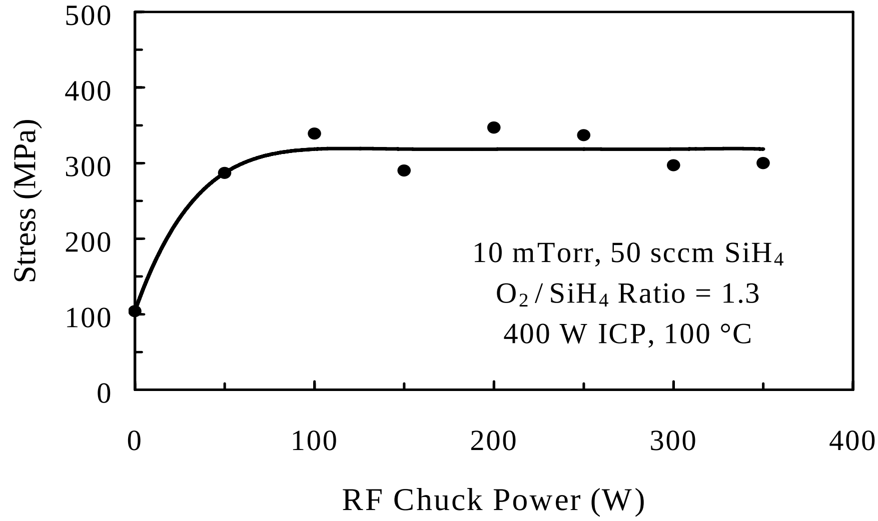

Figure 6. Film Stress of HDPCVD oxide as a function of rf chuck power. The stress is compressive for all films.

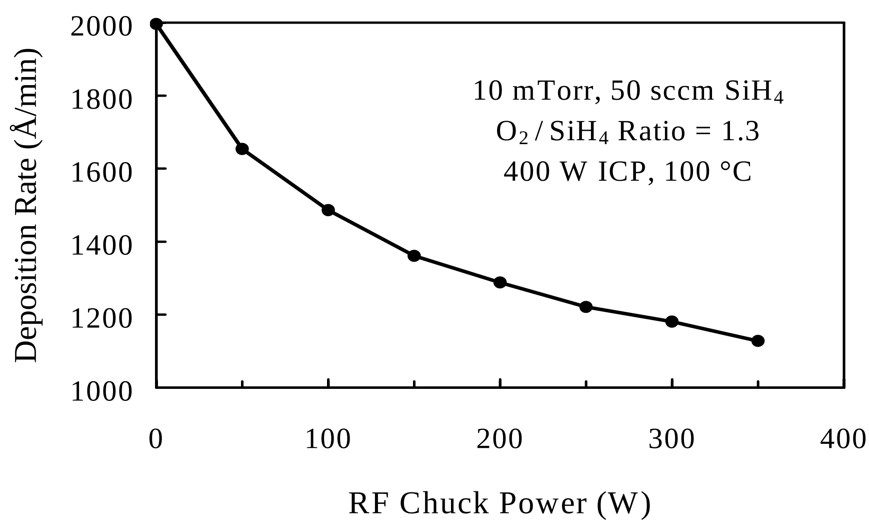

Figure 7. Deposition rate of HDPCVD oxide as a function of rf chuck power.

As a final comment on the HDPCVD SiO_2 work, it worthwhile discussing further the significance of the BHF etch rate data. The BHF etch rate of 1300 Å/min for these HDPCVD films compares favorably to value of about 800 Å/min for thermally-grown SiO_2. This implies that the quality of HDPCVD SiO_2 is very good. It is significant improvement over PECVD SiO_2. The measured BHF etch rate for 100 °C PECVD SiO_2 prepared from a standard (SiH_4 + N_2O + N_2) chemistry is in excess of 15,000 Å/min.

Silicon Nitride

In this section, the results of an investigation of the effects of N_2 / SiH_4 gas ratio and rf chuck power on the material properties of SiN_x are presented. The particular properties investigated were deposition rate, stress, refractive index, and BHF etch rate. Films with a refractive index of between 1.95 to 2.05, a low BHF etch rate, and a low compressive stress are desirable.

Figures 8, 9, and 10 summarize the dependence of the film properties on the N_2 / SiH_4 ratio. The deposition rate was about 500 Å/min. The thickness uniformity was ±4 % across the wafer. The refractive index decreases with increasing N_2 / SiH_4 ratio from 2.3 at a ratio of 0.5 to about 1.8 at a ratio of 0.95. A refractive index of 2.0 is achieved at a N_2 / SiH_4 ratio of 0.7. Both the BHF etch rate and the film stress increase monotonically with increasing N_2 / SiH_4 ratio. For a N_2 / SiH_4 ratio of 0.7, the BHF etch rate is about 1000 Å/min while the stress is about 300 MPa and compressive in nature.

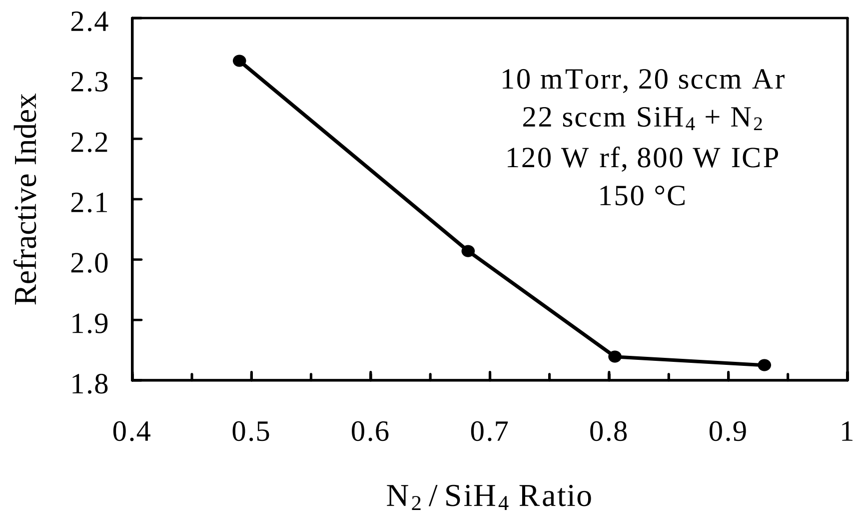

Figure 8. Refractive index of HDPCVD nitride as a function of N_2 / SiH_4 ratio.

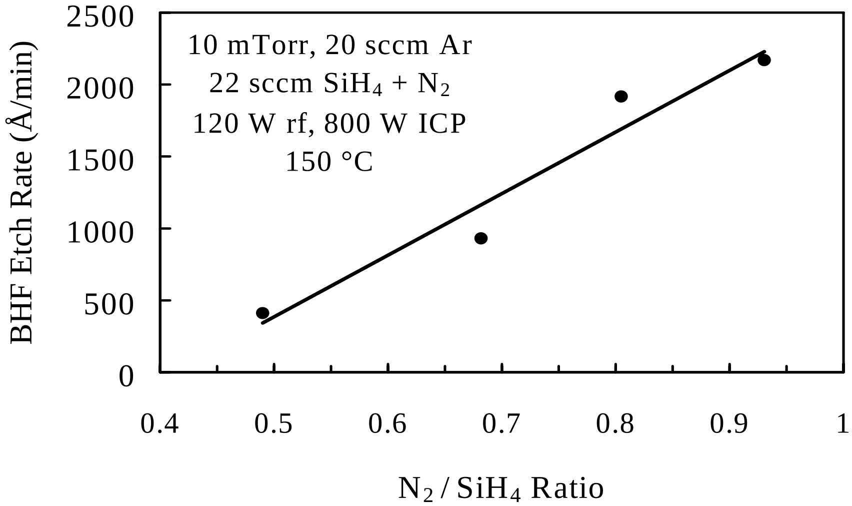

Figure 9. Variation of wet-etch rate of HDPCVD nitride with N_2 / SiH_4 ratio.

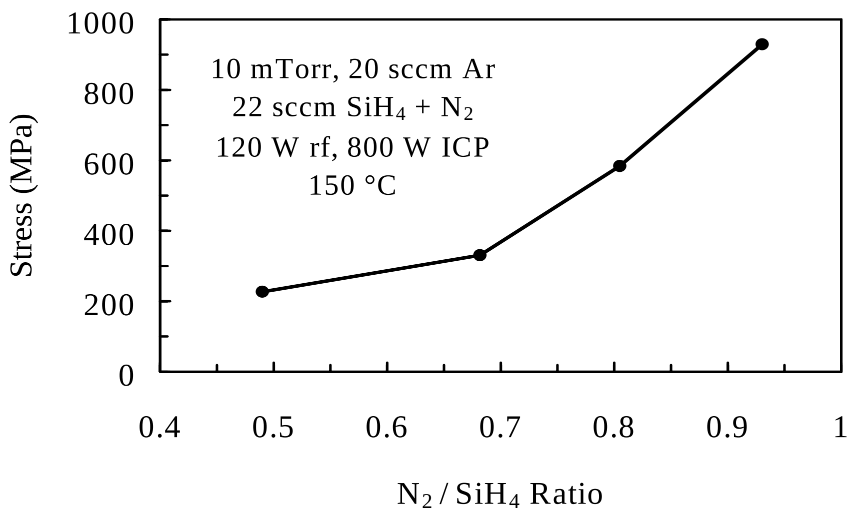

Figure 10. Film stress of HDPCVD nitride as a function of N_2 / SiH_4 ratio. The stress is compressive for all films.

Figures 11-14 summarize the effect of rf chuck power on the measured film properties. All the films were deposited using the optimum N_2 / SiH_4 ratio of 0.7. In Figure 11, the deposition rate as a function of rf chuck power is shown. The deposition rate decreases monotonically with increasing rf chuck power. The typical deposition rate was in the range of 400 - 600 Å/min.

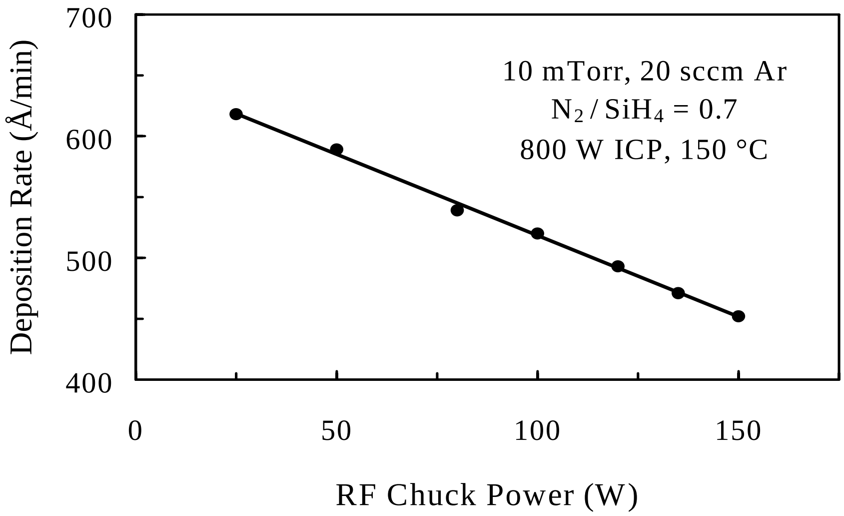

Figure 11. Deposition rate of HDPCVD nitride as a function of rf chuck power.

Figures 12 and 13 show the refractive index and stress data. The refractive index increases with increasing rf chuck power from 1.95 at 25 W to about 2.05 at 150 W. This behavior implies that raising the rf chuck power leads to Si-rich nitride films. This suggests that dissociation of SiH_4 into neutrals compared to N_2 increases with rf chuck power. As shown in Figure 13, the film stress of all the SiN_x films was compressive in nature. The stress decreases with increasing rf chuck power. At 25 W rf chuck power, the stress was as high as 900 MPa. The lowest stress of 300 MPa is achieved at 125 W. If we assume that less than 500 MPa is acceptable for SiN_x, the operation window for rf chuck power is 80 W to 120 W.

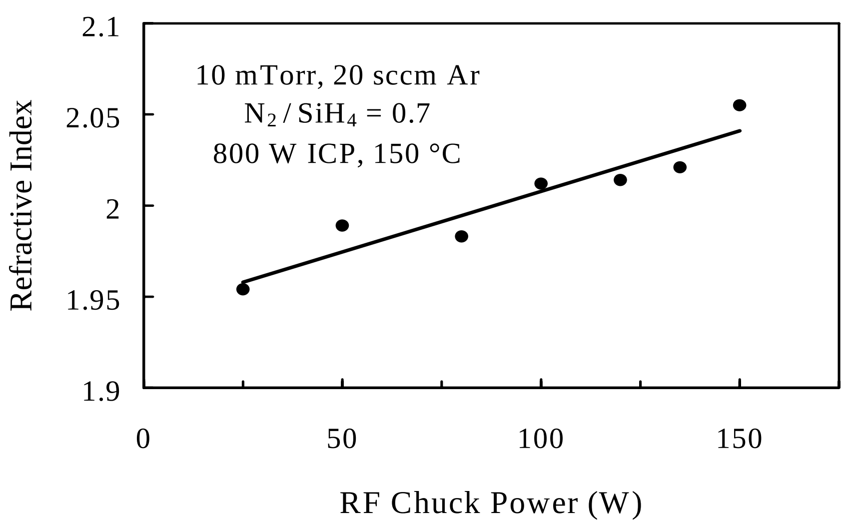

Figure 12. Refractive index of HDPCVD nitride as a function of rf chuck power.

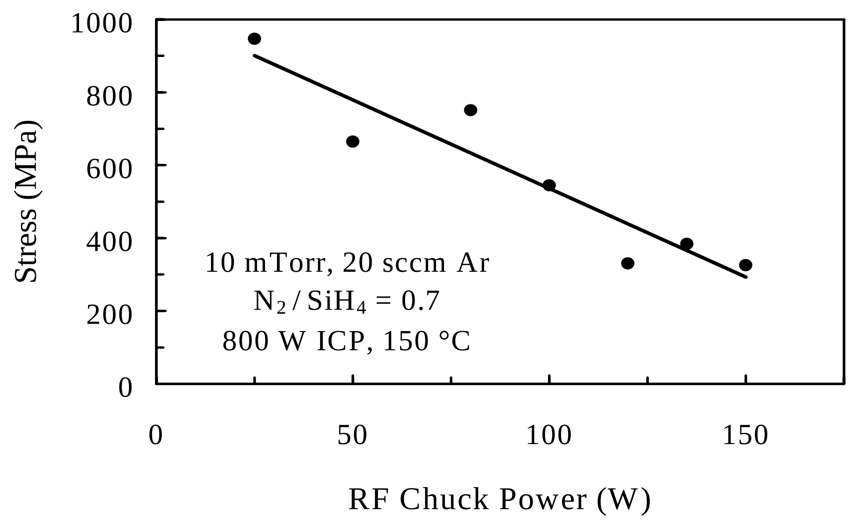

Figure 13. Film Stress of HDPCVD nitride as a function of rf chuck power. The stress is compressive for all films.

Figure 14 shows the BHF etch rate data for these films. The BHF etch rate is decreased by about a factor of 2 with increasing rf power. This may be due in part to the change in the stoichiometry as reflected in the refractive index data presented in Figure 12.

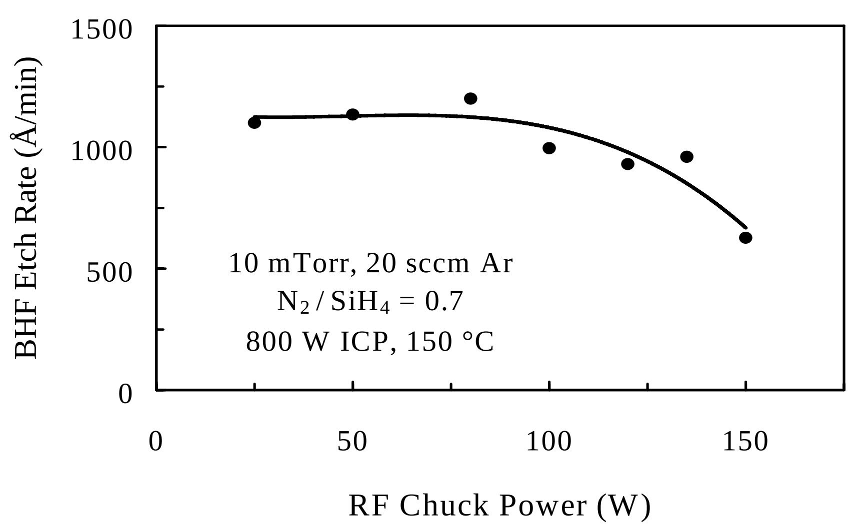

Figure 14. Variation of wet-etch rate of HDPCVD nitride with rf chuck power.

Wet-etch rate measurements have also been made on SiN_x films deposited by PECVD. A series of films was deposited using a standard (SiH_4 + NH_3 + N_2) process chemistry. The deposition temperature was varied from 100 to 300 °C. For comparison, a similar series of HDPCVD films was prepared from (SiH_4 + N_2 + Ar). In Figure 15, the BHF etch rate results for the PECVD and HDPCVD SiN_x films are presented. As expected, for both HDPCVD and PECVD, raising the deposition temperature lowers the BHF etch rate. However, the most notable aspect of the results is that low temperature SiN_x prepared by HDPCVD has a significantly lower BHF etch rate. For example, at 100 °C, the BHF etch rate of HDPCVD films is about 1000 Å/min compared to about 11,000 Å/min for PECVD films. For deposition temperatures less than 200 °C, HDPCVD SiN_x is of superior quality to PECVD SiN_x. The lower BHF etch rate implies that the HDPCVD films are more dense and contain less hydrogen [24]. The use of N_2 instead of NH_3 probably contributes to the lower hydrogen content in the HDPCVD films.

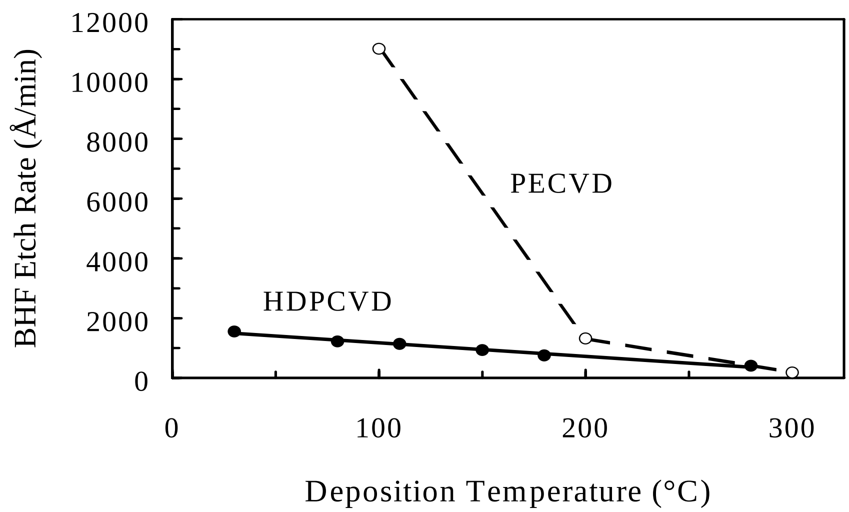

Figure 15. Comparison of the BHF etch rates of HDPCVD and PECVD nitride *versus* deposition temperature. The refractive index of the SiN_x films is 2.0.

CONCLUSIONS

In summary, the work in this paper has demonstrated that high quality SiO_2 and SiN_x films can be deposited by the HDPCVD technique at temperatures less than 200 °C. Future work will involve a study of the electrical and structural properties of these films. This will include a determination of the hydrogen content and bonding in these films.

ACKNOWLEDGMENTS

The authors gratefully acknowledge the technical support from Mr. L. Heckerd and Mr. R. McAfee.

REFERENCES

1. R. Williams, *Modern GaAs Processing Methods*, p. 153, Artech House, Inc., Norwood MA (1990).

2. U. K. Chakrabarti, *Indium Phosphide and Related Materials: Processing, Technology, and Devices*, A. Katz, Editor, p. 337, Artech House, Inc., Norwood MA (1992).
3. J. Etrillard, F. Heliot, P. Ossart, M. Juhel, G. Partiarche, P. Carcenac, C. Vieu, M. Puech and P. Maquin, *J. Vac. Sci. Technol. A*, **14,** 1056 (1996).
4. E. Berg and S. W. Pang, *J. Vac. Sci. Technol. B*, **15,** 2643 (1997).
5. F. Ren, J. W. Lee, C. R. Abernathy, S. J. Pearton, C. Constantine, C. Barratt and R. J. Shul, *Appl. Phys. Lett.*, **70**, 2410 (1997).
6. J. W. Lee, C. R. Abernathy, S. J. Pearton, F. Ren and R. J. Shul, C. Constantine and C. Barratt, *Solid-State Electron.*, **41**, 829 (1997).
7. J. W. Lee, S. J. Pearton, F. Ren, R. F. Kopf, J. M. Kuo, R. J. Shul, C. Constantine and D. Johnson, *J. Electrochem. Soc.*, **145**, 4036 (1998).
8. Y. B. Hahn, J. W. Lee, K. Mackenzie, D. Johnson, D. Hays, C. R. Abernathy and S. J. Pearton, *Electrochemical and Solid-State Lett.*, **1**, 230 (1998).
9. J. W. Lee, K. D. Mackenzie, D. Johnson, R. J. Shul, S. J. Pearton, C. R. Abernathy and F. Ren, *Solid-State Electron.*, **42**, 1015 (1998).
10. J. W. Lee, K. D. Mackenzie, D. Johnson, R. J. Shul, S. J. Pearton, C. R. Abernathy and F. Ren, *Solid-State Electron.*, **42**, 1021 (1998).
11. J. W. Lee, K. D. Mackenzie, D. Johnson, R. J. Shul, S. J. Pearton, C. R. Abernathy and F. Ren, *Solid-State Electron.*, **42**, 1027 (1998).
12. J. Hopwood, *Plasma Sources Sci. Technol*., **1**, 109 (1992).
13. *High Density Plasma Sources*, O. A. Popov, Editor, Noyes Publications, Park Ridge, NJ (1995).
14. T. V. Herak, T. T. Chau, D. J. Thomson, S. R. Mejia, D. A. Buchanan and K. C. Kao, *J. Appl. Phys.*, **65**, 2457 (1989).
15. K. L. Seaward, J. E. Turner, K. Nauka and A. M. E. Nel, *J. Vac. Sci. Technol. B*, **13**, 118 (1995).
16. M. Firon, M. C. Hugon, B. Agius, Y. Z. Hu, Y. Wang, and E. A. Irene, *J. Vac. Sci. Technol. B*, **14**, 2543 (1996).
17. F. Ren, J. LaRoche, T. Anderson, S. J. Pearton, J. W. Lee, D. Johnson, J. R. Lothian, J. Lin, J. S. Weiner, R. J. Shul and C. S. Wu, *Electrochemical and Solid-State Lett.*, **1**, 279 (1998).
18. F. Delmotte, M. C. Hugon, B. Agius and J. L. Courant, *J. Vac. Sci. Technol. B*, **15**, 1919 (1997).
19. B. F. Hanyaloglu and E. S. Aydil, *J. Vac. Sci. Technol. A*, **16**, 2794 (1998).
20. M. J. Kushner, *J. Appl. Phys*., **74**, 6538 (1993).
21. E. Meeks, R. S. Larson, P. Ho, C. Apblett, S. M. Han, E. Edelberg and E. S. Aydil, *J. Vac. Sci. Technol. A*, **16**, 544 (1998).
22. R. Chebi and S. Mittal, *Proc. of the Eighth International IEEE VLSI Multilevel Interconnection Conference*, Santa Clara, CA. (IEEE, New York, 1991), p.61.
23. P. Shufflebotham, M. Weise, D. Pirkle and D. Denison, *Mater. Sci. Forum*, **140-142**, 255 (1993).
24. J. Kanicki, *Mat. Res. Soc. Symp. Proc.*, **118**, 671 (1988).